NUMERICAL SIMULATION OF THE PROGRESSIVE FLOODING OF A BOX-SHAPED BARGE

Santos, T.A., Dupla, P., Guedes Soares, C.
Centre for Marine Technology and Engineering (CENTEC)
Technical University of Lisbon, Instituto Superior Técnico
Lisbon - Portugal

ABSTRACT

Numerical simulation methods capable of predicting the progressive flooding of passenger and cargo ships and the time required for such extreme events as sinking or capsize are still relatively uncommon. This paper presents a numerical method capable of describing the progressive flooding of ships taking in consideration complex subdivision arrangements. Numerical results are shown for the progressive flooding of the ITTC box-shaped barge. Multiple types of flooding and internal openings are considered, including complex cross-flooding, up-flooding and down-flooding situations. Comparison is made with experimental results aiming at validating the numerical simulation method and conclusions are drawn.

Keywords: *damage stability, progressive flooding, simulation*

1. INTRODUCTION

Large passenger ships carrying substantial numbers of passengers and crews onboard are widely operated in cruises and short sea routes. IMO started a task on safety of these ships in 2001 and the SLF sub-committee decided to study the time to sink for all damage cases with probability of survival below 1. This work was part of the regulatory gaps identified at the time, mainly related to survivability of the ship, structural integrity after damage and raking damages, see IMO-SLF (2001). Studies within IMO then identified as required for accurate time to sink or time to capsize numerical estimates the appropriate modelling of partially watertight bulkheads, pipes and ducts, leakage rates and permeabilities. This is especially important due to the complicated arrangements of passenger ships. IMO-SLF (2002) also indicates that time dependent flooding calculations should be compared to experimental tests in order to validate the numerical models.

Veer et al. (2002) carried out work on the numerical simulation of the flooding of a large passenger ship whose internal layout comprised numerous compartments and connections. Simulations were carried out in irregular seas typical of the North Atlantic and the time-to-sink determined for various sea states in given damage conditions. A well-defined survival boundary, similar to the ro-ro ship capsize boundary was found.

Ikeda and Katayama (2003) presented results of model experiments for a damaged large passenger ship. Various types of damage openings were studied leading to flooding up to four compartments. The behaviour of the ship in the intermediate stages of flooding depends significantly on the arrangement of the flooded decks, with raking damages causing larger heel angles in the intermediate stages of flooding.

Veer et al. (2004) carried out further numerical simulations of the behaviour of a large passenger ship which indicated that in extreme sea states the accurate modelling of details of openings between compartments and of the protection of downflooding points becomes less important when predicting the time to sink. The scatter of the time-to-sink increases with the increasing of the wave height. More simulations then become necessary to determine the survivability boundary with respect to the selected criterion.

Valanto (2002) has also carried out a numerical study on the survivability of a ro-pax ship, aiming at determining the survival time. The main idea is to design the ship so that the evacuation (or rescue) is possible in the time prior to capsizing. Systematic results for various ships and different damage conditions could also in the future be used to define a safety standard for ships carrying passengers. The study also concluded that a considerable number of simulations is necessary to appropriately predict the mean survival time.

Ruponen (2006) has also carried out experimental work within the scope of the IMO large passenger ship safety initiative, aiming at improving knowledge on the effects of semi-watertight structures and internal boundaries on the survivability of ships, with particular focus on progressive flooding. The same author developed a numerical model to deal with complex flooding cases including the possibility of air trapping in some compartments, as reported in Ruponen (2006).

Subsequently, as reported by Walree and Papanikolaou (2007), and now within the scope of ITTC, a benchmark study was carried out on the flooding of a box-shaped barge including the comparison of numerical results with experimental results. Several participants used different codes to simulate the flooding of the barge. Most codes use hydraulic models to simulate the flow of water between different compartments. A number of differences were identified between the numerical results and the experimental results, namely difficulties in accounting thickness of model walls, partially ventilated compartments, discharge coefficients and in the integration methods used to calculate the water level and air pressure in time domain. The steady state condition of all specified tests is reasonably well predicted by the benchmarking codes but the prediction of the flooding rates and transient phenomena is less satisfactory.

The application of these numerical models in reasonably predicting time-to-sink appears feasible for ships having relatively simple internal geometry and interrelation of flooded compartments under calm water conditions. For more complex geometries and in waves the prediction of time-to-sink will be less reliable.

A second phase of this research, reported by Walree and Carette (2008), aims at establish current capability and weaknesses in predicting, qualitatively and quantitatively, the time-to-flood for a typical passenger ship hull form with complex configuration of internal compartments.

Due to no experimental results for existing passenger ships being made available, only a comparison of simulation results was carried out. Only two participants in the study could complete the scheduled tests, indicating the difficulties of calculation with complicated compartment layout for current cruise ships.

Results showed that for the most severe flooding and sea conditions considerable differences appear for the predicted time-to-flood.

This paper presents numerical results of a code reported in Santos and Guedes Soares (2001) and Santos et al. (2002). This time domain code uses a panel method to calculate the hydrostatic forces acting in the ship's hull and in the flooded compartments and also can calculate the hull girder global loads as presented in Santos and Guedes Soares (2008). The results in this paper were obtained for the

barge studied by Ruponen (2006) and correspond to the test cases defined for the first phase of the ITTC benchmark study.

2. NUMERICAL MODEL

2.1 Equations of Motion

The ship motions are expressed in the coordinate system shown in Figure 1.

The equations describing the ship motions are, essentially, similar to those presented by Santos et al. (2002):

$$\sum_{j=2}^{6}(M_{ij}+A_{ij})\ddot{X}_j(t)+B_{ij}\dot{X}_j(t)+F_j(t)=F_i^E(t)+F_i^{AL}(t) \quad (1)$$

for i = 2,…,6 where:

M_{ij} represents the mass matrix,

A_{ij} and B_{ij} represent the radiation coefficients,

F_i represents the hydrostatic forces,

F_i^E represents the wave excitation forces (diffraction forces plus Froude-Krylov forces),

F_i^{AC} represents the floodwater forces.

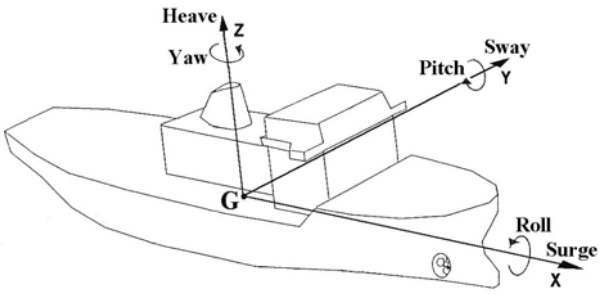

Figure 1. Coordinate System for Ship Motions.

The hydrostatic forces are calculated over the instantaneous wetted surface taking into account the ship's motions. These forces are calculated using the hydrostatic pressure integration technique described by Santos and Guedes Soares (2001). The viscous roll damping is approximated by a linearized coefficient, which is estimated using the results of model experiments. Given that the motions in this study are relatively slow due to the absence of waves, damping is not a major concern.

2.2 Flooding Model

The forces and moments acting in the ship as a result of floodwater are calculated under the following assumptions:

- water flows in a quasi-static way inside each compartment,
- the waterplane in each flooded compartment is flat and horizontal in each instant.

Taking into account these assumptions, knowing how much water is inside each compartment in each moment, the forces and moments caused on the ship by the floodwater can be calculated using:

$$\begin{aligned} F_3^{AL} &= \sum_{j=1}^{Ncomp} M_{wj}\rho_s g \\ M_4^{AL} &= \sum_{j=1}^{NComp} M_{wj}\rho_s g(y_G - y_{Mwj}) \\ M_5^{AL} &= \sum_{j=1}^{NComp} M_{wj}\rho_s g(x_G - x_{Mwj}) \end{aligned} \quad (2)$$

where M_{wj} represents the volume of water in the j flooded compartment and $Ncomp$ represents the number of flooded compartment.

The water inside each compartment is calculated using an hydraulic model which, at each time step, adds or subtracts an amount of water. Having obtained the new value for the total amount of water inside the compartment, the level of water is calculated iteratively. As a result of this iterative process, the coordinates of the centre of the floodwater are obtained. The process is repeated for each flooded compartment and the results are used in equation (2).

The flow of water between two interconnected compartments depends on the difference of water levels between both compartments. Bernoulli's theorem is first used:

$$h_{out} + \frac{P_{atm}}{\rho g} + 0 = h_{in} + \frac{P_{atm}}{\rho g} + \frac{v^2}{2g} \quad (3)$$

where h_{in} *and* h_{out} are the water levels in both compartments, P_{atm} is the atmospheric pressure, ρ is the specific mass of the water, g is the acceleration of gravity and v is the water velocity, which can then be obtained through:

$$v = \sqrt{2g(h_{out} - h_{in})} \quad (4)$$

The flow rate is then obtained through:

$$Q = \iint_A K\sqrt{2g(h_{out} - h_{in})}dA \quad (5)$$

where K is the hydraulic coefficient, obtained experimentally. The flow rate can then be multiplied by the time step and the amount of water which enters or leaves the compartment is obtained.

The hydraulic coefficient influences the flow rate and the amounts of water in the different flooded compartments in the time domain. Typical values for hydraulic coefficients applicable to the problem of progressive flooding of ships are not abundant in the open literature. In that sense, studies such as that of Ruponen et al. (2006) are very valuable and point towards hydraulic coefficients between 0.6 and 0.8, with 0.7 being a common value. This magnitude of variation of the hydraulic coefficient is not susceptible of affecting significantly the transient stages of flooding.

Currently, the theoretical model considers all compartments to be fully ventilated, but some other models like that of Xia et al. (1999) and Ruponen (2007) take into account air flows and entrapped air, phenomena which are of interest only in specific situations.

3. MAIN CHARACTERISTICS OF BARGE

3.1 General Dimensions

The barge which was used in the experimental programme is a box shaped barge as shown in Figure 2.

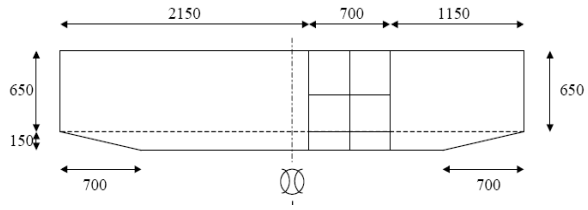

Figure 2. Barge profile.

Table 1. shows the barge main dimensions.

Table 1. Barge main dimensions.

Lenght over all:	4,000 m
Breath:	0,800 m
Height	0,800 m
Design draft:	0,500 m
Block coefficient at design draft:	0,906 m
Volume of Buoyancy	1,450 m³

In this barge there is a block for the flooded compartments, inside which there are 8 floodable compartments: DB1, DB2, R11, R21, R21P, R21S, R12 and R22. Figures 3 and 4 show the cross section and profile of the floodable part of the barge.

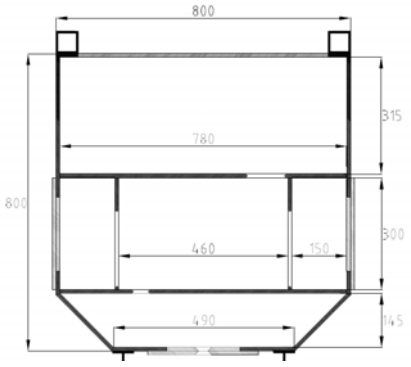

Figure 3. Cross section of damaged part of barge with main dimensions.

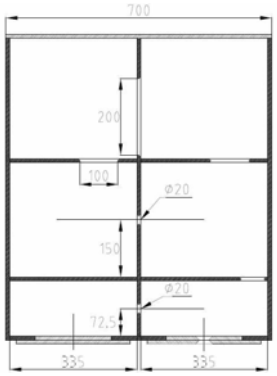

Figure 4. Profile of damaged part of barge with main dimensions.

The initial conditions when the barge is floating freely are given in Table 2.

Table 2. Barge initial condition.

Draft	0,500 m
Heel	0,0°
Trim	0,0°
Vertical center of Buoyancy, KBo	0,270 m
Initial metacentric radius, BoMo	0,118 m
Initial metacentric height, GMo	0,110 m
Vertical center of gravity, KG	0,278 m
Inertia Ixx	0,171 m^4

3.2 Characteristics of Openings

All of the compartments are connected through internal openings. Figure 5 shows the location of all openings. Basically there are openings (larger or smaller) in the double bottom to allow water inside the barge. DB2 is connected to R21 through a orifice in the double bottom. R21 is in turn connected to R21S and R21P through large vertical openings. R21 also is connected to R11 using a circular hole half way between double bottom and deck. R21 is also connected to R22 (above it) and R11 is connected to R12 in a similar way. Generally, water floods first the double-bottom, then up floods R21, R21P and R21S and finally R11, where R11 and R21 are full, water up floods R12 and R22 respectively. There is also a door type opening connecting R12 and R22. This is open only in one experiment. In the last experiment, a side opening leading to R21S is used to flood the barge, instead of the usual bottom opening.

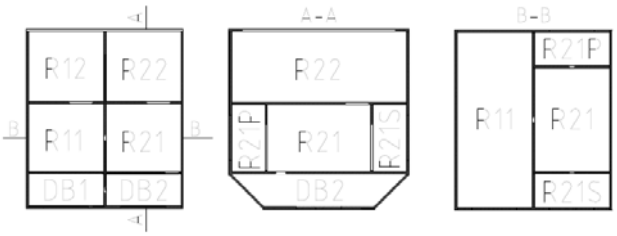

Figure 5. Location of openings.

Regarding the damage openings, there are two types of damage openings in the bottom as shown in Table 3.

Table 3 Damage hole

	Breath	Height	Area
Large damage hole	60 mm	40 mm	24,0 cml
Small damage hole	25 mm	25 mm	6,25 cml

All of the openings were tested before the experiments and the hydraulic coefficients were measured, with the results being given in Table 4. These coefficients were used in the numerical simulations shown below.

Table 4. Damage holes and hydraulic coefficients.

Connection	Size	Hydraulic coeff
SEA-DB1	60 mm × 40 mm	0.78
SEA-DB2	25 mm × 25 mm	0.83
SEA-R21S	60 mm × 40 mm	0.78
DB1-DB2	Circ. hole, D = 20 mm	0.8
DB2-R21	60 mm × 40 mm	0.78
R21-R21S	20 mm × 200 mm	0.75
R21-R21P	20 mm × 200 mm	0.75
R21-R11	D = 20 mm	0.80
R21-R22	100 mm × 100 mm	0.72
R11-R12	100 mm × 100 mm	0.72
R12-R22	80 mm × 200 mm	0.72
R21S-ATM	Vent. pipe, D = 7 mm	0.67
R21P-ATM	Vent. pipe, D = 7 mm	0.67

4 COMPARISON WITH EXPERIMENTS

4.1 Experimental Programme

The floating position of the model was measured with a camera-based solution measuring the 6D movements of object in space. There were also 9 sensors, one in each compartment and 2 in the DB2 compartment, to measure the water height in every flooded compartment. The over-pressures are measured

in the double bottom compartments with pressure difference gauges.

Five different tests with different conditions were carried out as shown in Table 5. In every the tests, all compartments are flooded except the last one, where the bottom compartments are not flooded. The watertight door between R12 and R22 is open only in test3.

Table 5. Test presentation.

Name:	Damage Case:	WT-door:	Special:
Test01	Bottom comp2 small	closed	fixed floating position
Test02	Bottom comp2 small	closed	
Test03	Bottom comp2 small	open	
Test04	Bottom comp2 large	closed	
Test05	Bottom comp1 large	closed	
Test06	Side comp2 large	closed	Double bottom dry

For the five experiments, the barge's trim, sinkage, water heights and overpressure were measured.

4.2 Comparison with Numerical Results

The experimental tests were simulated using the computer program described above and comparison with the numerical results is now presented. Test 1 is omitted as the barge is not freely floating but results for the other five tests are presented.

4.2.1 Test2

Figures 6 to 13 show the numerical and experimental results for test 2. Numerical simulation of flooding test 2 allows the following conclusions when compared to the experimental results:

- DB2 floods in a similar way but it becomes flooded faster,
- DB1 floods completely since no air is entrapped (compartment fully ventilated) and this responsible for the difference in water height which in the numerical results is located higher (4.4m instead of 5.1m),
- R21 floods in a similar way but starts flooding later, only after DB1 and DB2 are full,
- R21S and R21P flood in a similar way to R21, with a similar delay to experimental results,
- R11 starts flooding before R21 is full, as the opening is located half height of the compartments,
- R11 takes considerable time flooding, more than experimental results show,
- R12 starts flooding when R11 is full (1300s) and floods extremely rapidly in comparison with experimental results,
- R22 floods when R21 is full (500s) and the process is also much faster than in the experimental results,
- Note also as the water levels of all full compartments decrease slightly when R12 is flooded because the barge sinks when that compartment becomes flooded.

4.2.2 Test3

Figures 14 to 21 show the numerical and experimental results for test 3. Numerical simulation of flooding test 3 (equal to previous one but with watertight door between R12 and R22 open) allows the following conclusions when compared to the experimental results:

- Flooding of DB1 and DB2 is similar to test 2 and DB1 is again fully ventilated while in experimental results air is trapped,
- R21, R21S and R21P are flooded also in a similar way to test 2 but when R21 becomes full (slightly before 500s) water floods compartment R22 above and from there goes to R12 (almost immediately),
- R11 is first flooded from R21 after 300s and after 500s is flooded both from R21 and from R12, and this process is very fast,
- While R11 is flooded from R21 and R12 note as the water level in R12 and R22 actually decreases, and this process also exists in the experimental results but is slower and thus the water levels only fall slightly,

- As in test 2, the flooding of R12 and R22 is extremely fast compared to experimental results.

4.2.3. Test4

Figures 22 to 29 show the numerical and experimental results for test 4. Numerical simulation of flooding test 4 (equal to test 2 but with larger opening in bottom of compartment DB2) allows the following conclusions when compared to the experimental results:

- DB1, DB2, R21, R21P, R21S flood in a similar way to experimental results, but in general do so slower,
- DB1 shows the usual difference in water level due to absence of trapped air,
- R11 floods much slowly than in the experimental results, as also happens in Test 2,
- R21 starts flooding later than in the experimental results because R21 also becomes full later,
- R12 becomes flooded when R11 becomes full, and this happens much later than in the experimental results (1300s instead of 700s),
- Flooding of R12 and R22 is extremely fast in comparison to experimental results.

4.2.4. Test5

Figures 30 to 37 show the numerical and experimental results for test 4. Numerical simulation of flooding test 5 (equal to test 2 but with large opening in bottom of compartment DB1) allows the following conclusions when compared to the experimental results:

- DB1 and DB2 are flooded in a similar way to experimental results,
- R21, R21P and R21S are flooded much faster than in the experiments,
- R11 is also flooded slightly before than in the experimental results, but the rate of flooding is similar to the experimental results, R22 is flooded much earlier as R21 also becomes full much earlier,
- R12 is flooded at a similar time because R11 becomes full also at a time similar to the experimental results,
- The flooding of both R12 and R22 is extremely fast in comparison to experimental results.

4.2.5. Test6

Numerical simulation of flooding test 6 (no double bottom flooded and side opening to R21S) allows the following conclusions when compared to the experimental results:

- R21S, R21 and R21P are flooded in sequence and in a similar way to the experimental results, but do so slowly,
- R11 is flooded but slowly in comparison to experimental results,
- R12, in consequence of the delay in R11, is flooded much later than in the experimental results,
- R22 is flooded as R21 becomes full and this happens later than in the experimental results,
- Flooding of R12 and R22 is extremely fast in comparison to experimental results,
- Note the small differences in water levels in the different compartments in the final phase of flooding as no air is trapped in any compartment.

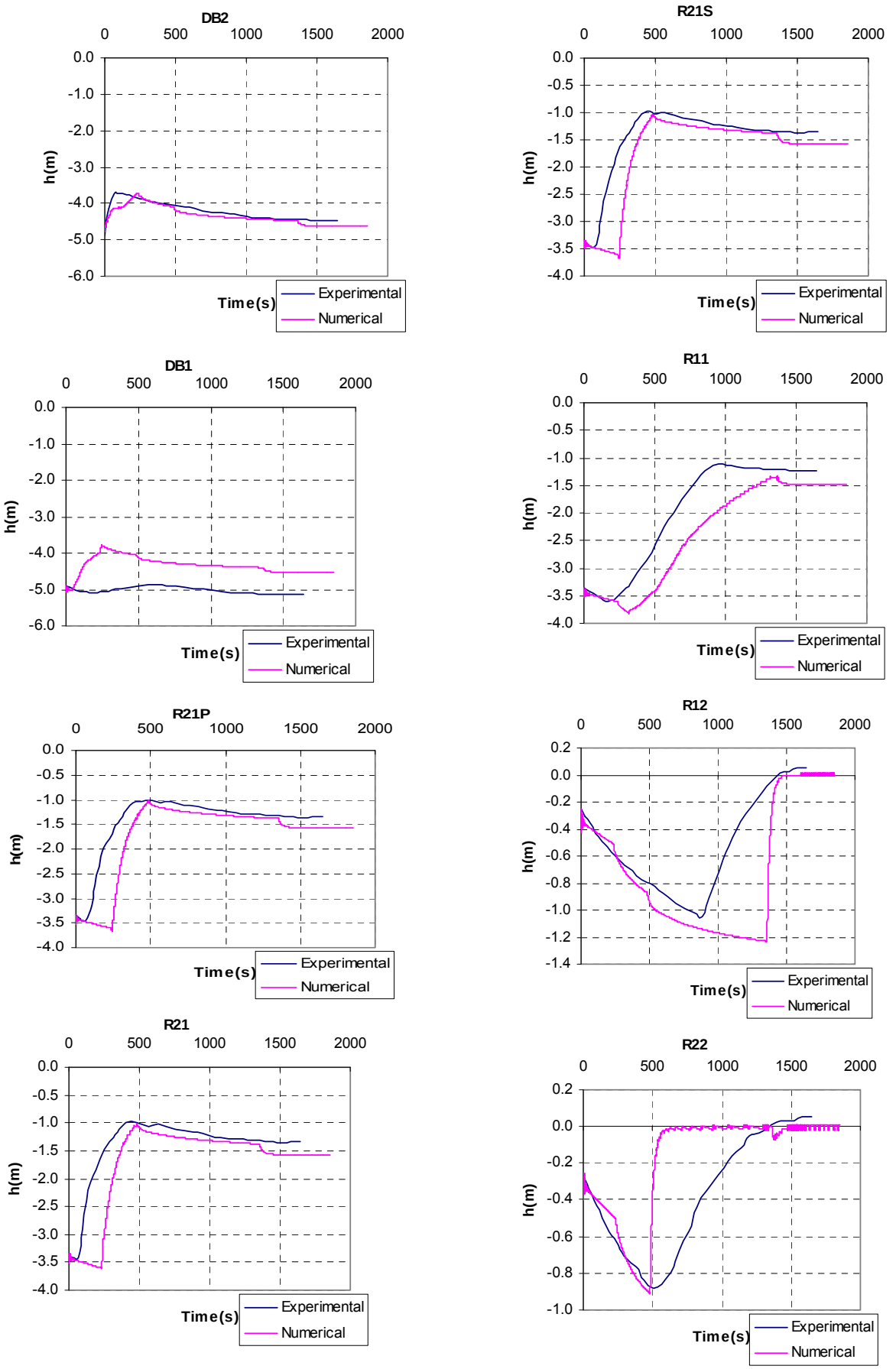

Figures 6 to 13. Results for Test.

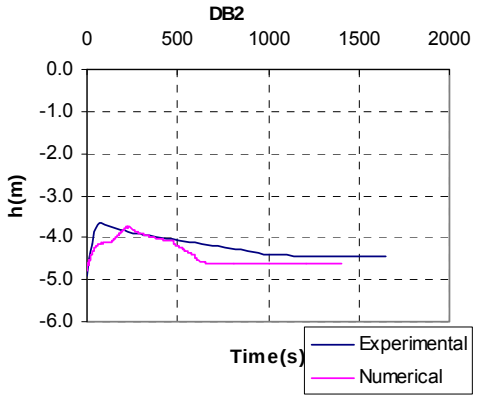

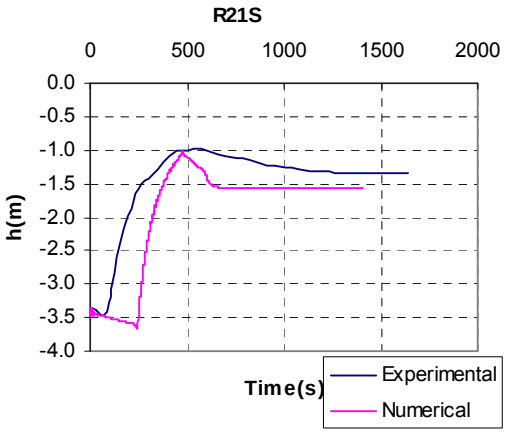

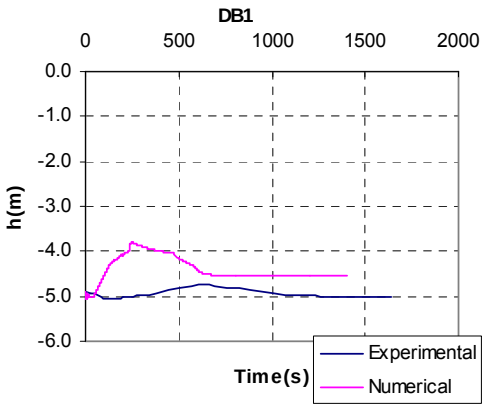

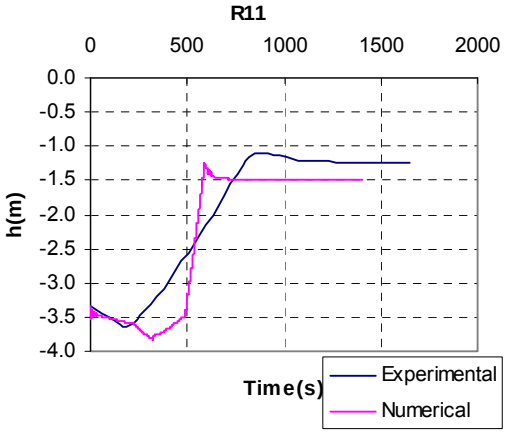

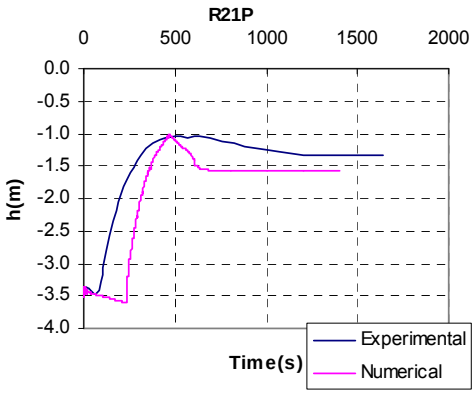

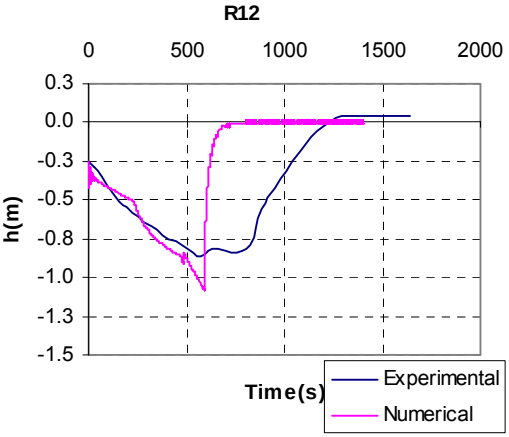

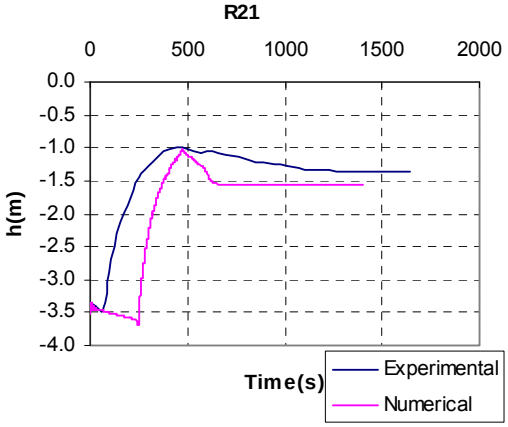

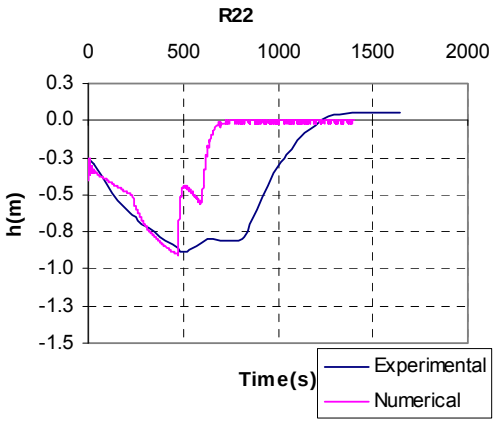

Figures 14 to 21. Results for Test 3.

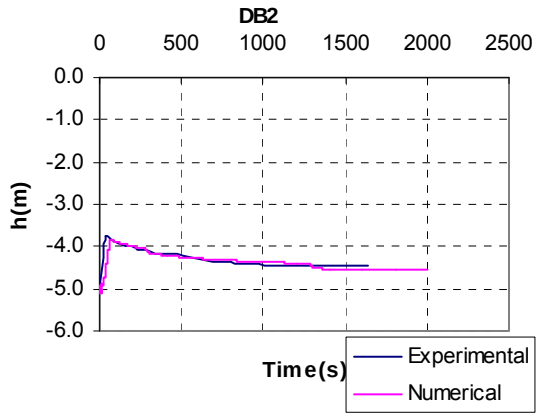

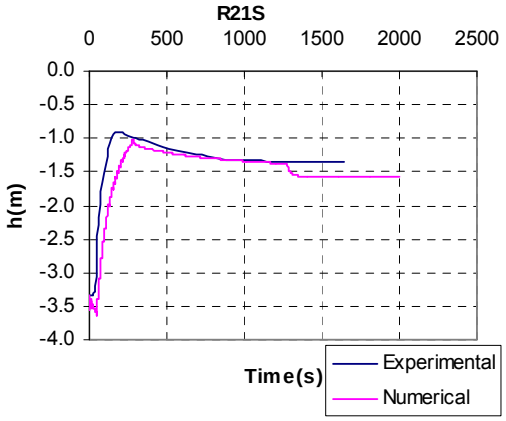

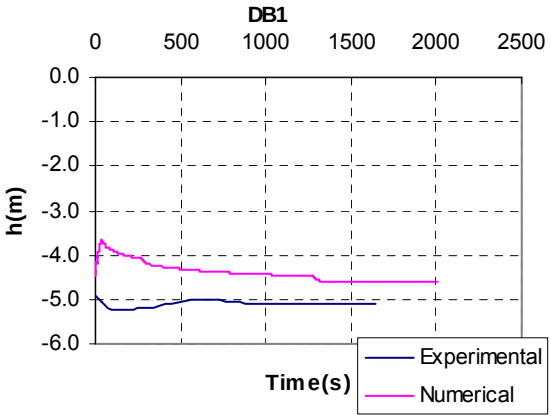

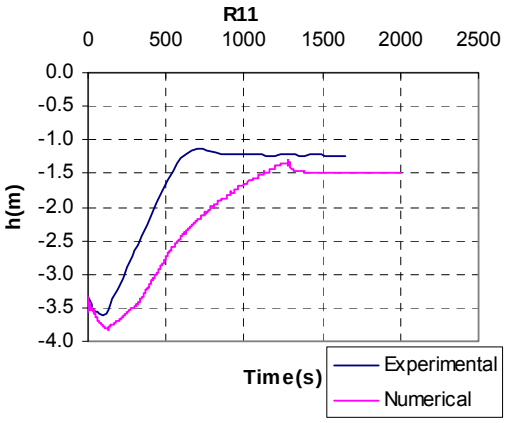

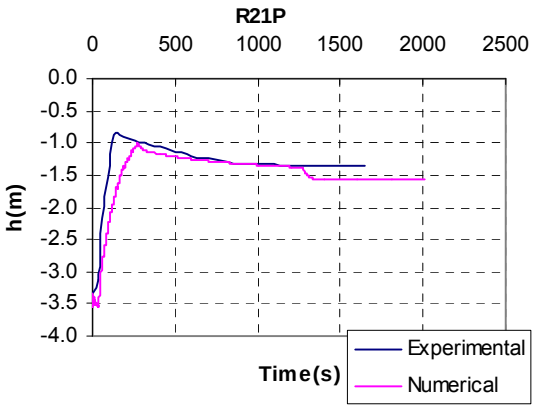

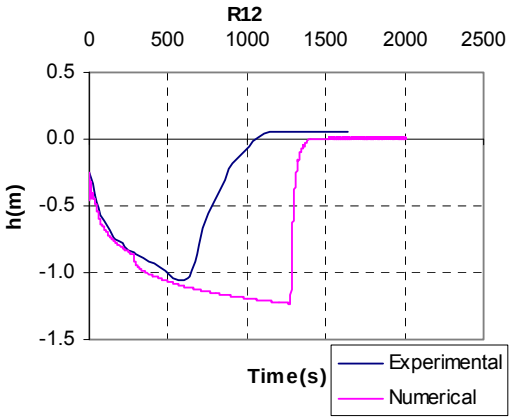

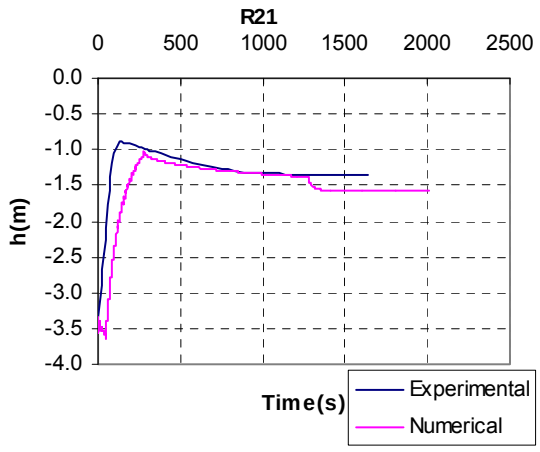

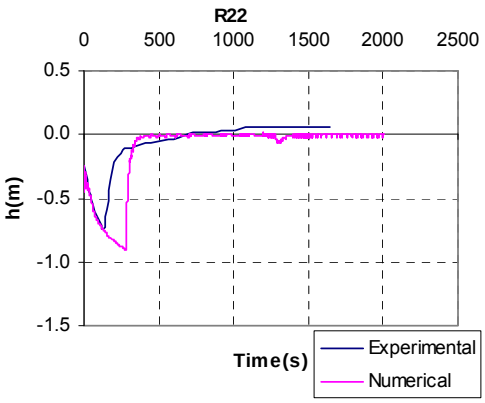

Figures 22 to 29 Results for Test 4

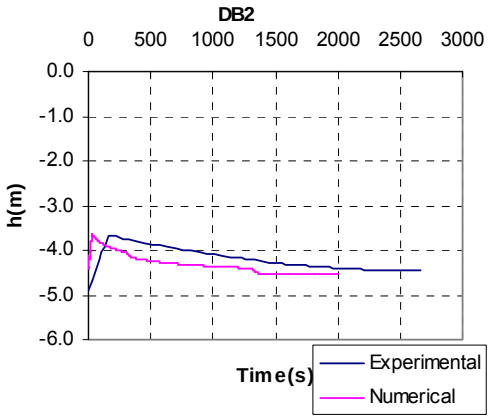

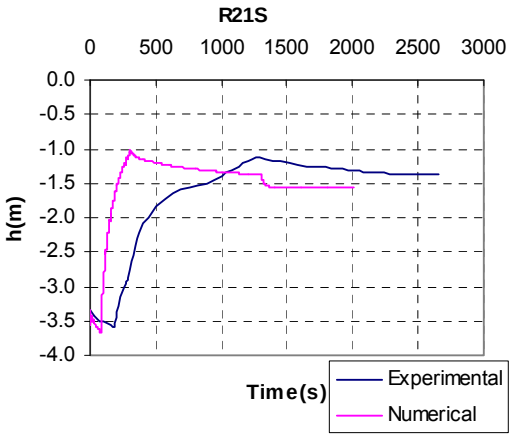

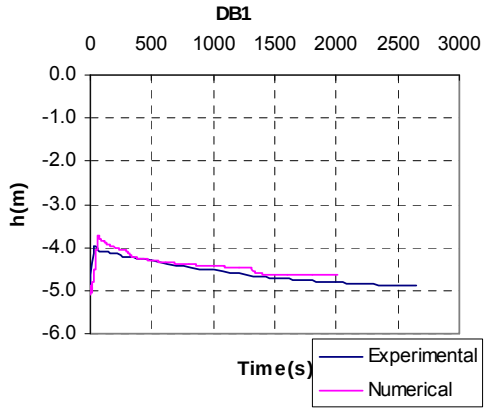

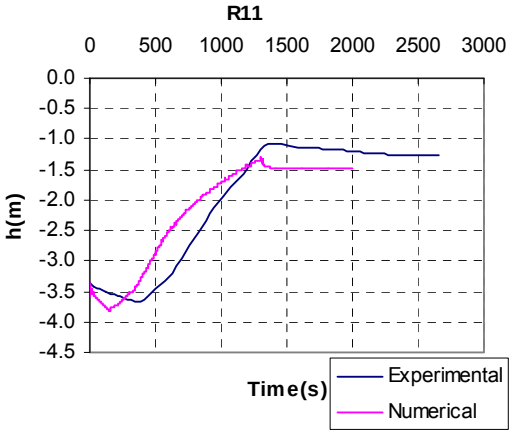

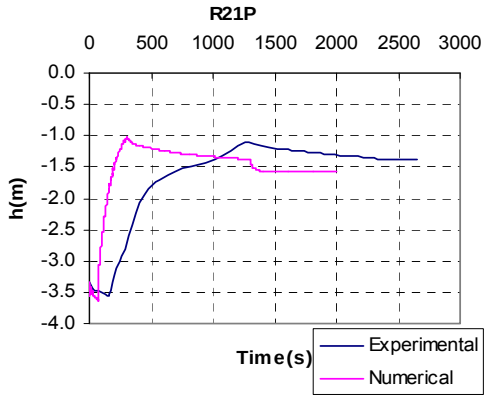

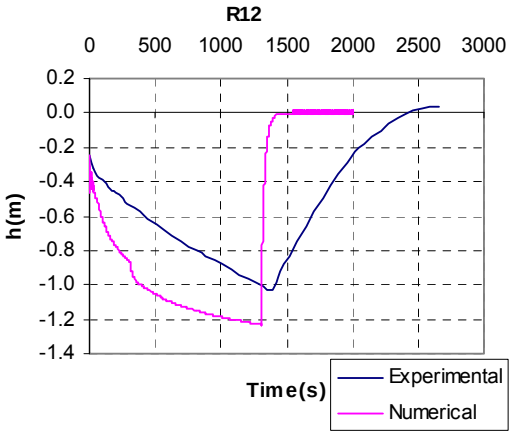

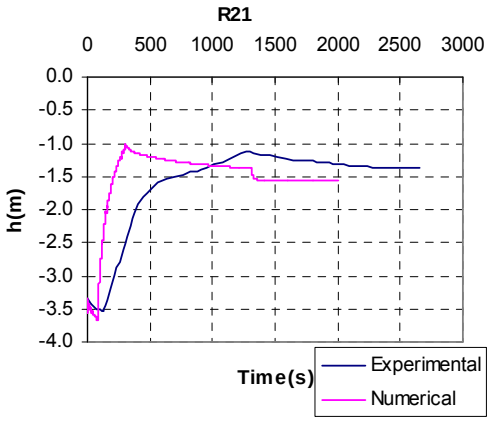

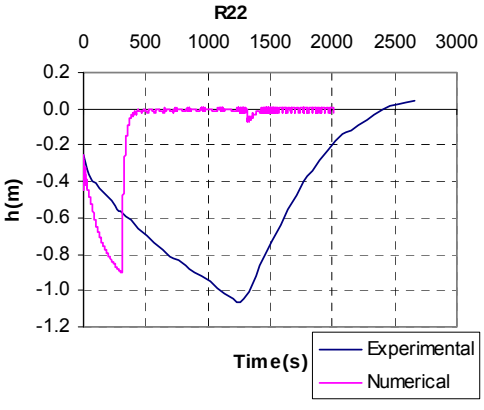

Figures 30 to 37 Results for Test 5

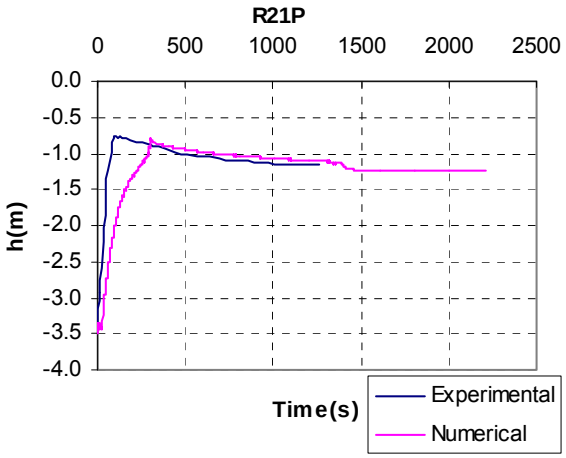

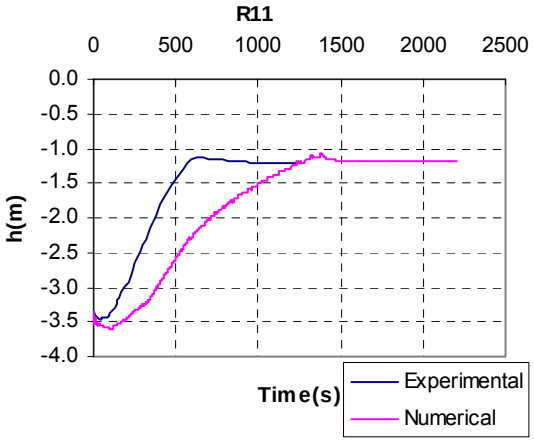

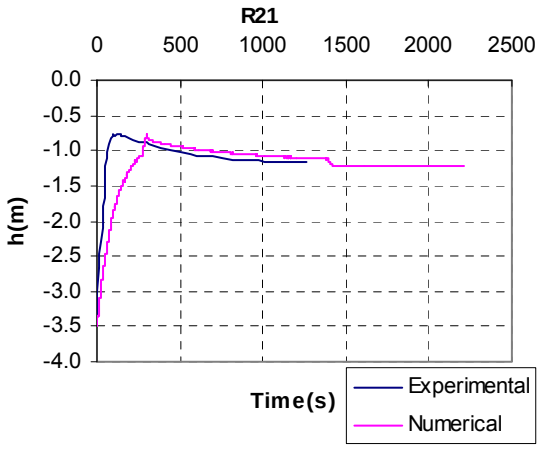

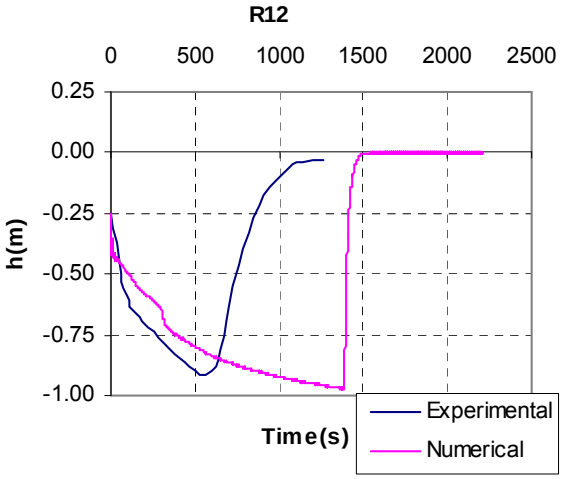

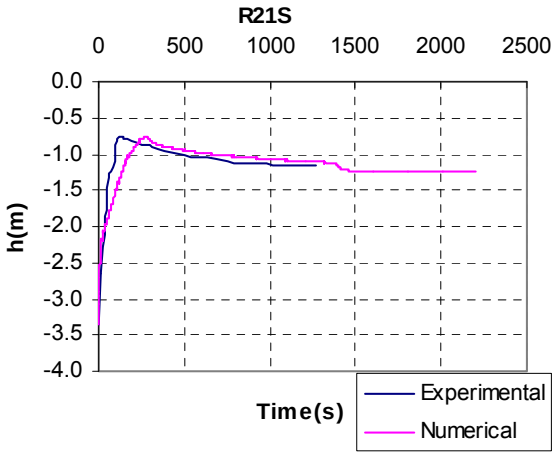

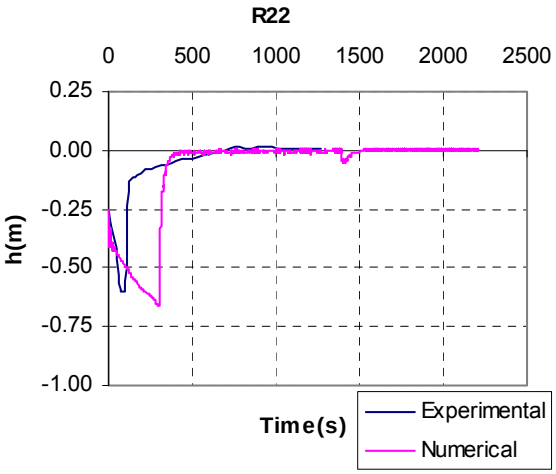

Figures 38 to 43. Results for Test 6.

5 CONCLUSIONS

This paper has presented numerical results of the simulation of a number of different flooding situations involving flooding from bottom and from side. The flooding cases involve progressive flooding across transverse and longitudinal bulkheads and decks. Openings between compartments are of various sizes and shapes. Air is trapped in one of the double bottoms. Hydraulic coefficients for the openings are taken from the results of the experiments.

Numerical results are qualitatively correct, showing complex phenomena also apparent in the experimental results. Final flooded equilibrium water levels are similar between numerical and experimental results except for the presence of air entrapped in double bottom leading to small discrepancies.

In spite of using the same hydraulic coefficients, the flow rates are different and lead to the compartments becoming full later or earlier. The time at which the compartments become full being different implies that compartments above are flooded later or earlier.

Flow rate is generally smaller than in experimental results for the opening between compartment R21 and R11. Flow rate is generally much higher in the numerical results for those openings located in the decks, which allow up flooding and downflooding. Differences in flow rates are the main problem causing differences between numerical and experimental results and can only be attributed to problems in the coding especially when considering more or less horizontal openings between compartments.

Air trapped is not currently modelled by the code but appears to cause only differences in water levels due to more water inside the barge. Probably some differences in the time domain also are caused by not considering air entrapment.

6 ACKNOWLEDGEMENTS

This paper has been prepared within the project “MARSTRUCT – Network of Excellence on Marine Structures”, (www.mar.ist.utl.pt/marstruct/), which is being funded by the European Union through the Growth program under contract TNE3-CT-2003-506141.

7 REFERENCES

Kat, J. de, Kanerva, M., Van’t Veer, R., Mikkonen, I. (2000), “Damage Survivability of a New Ro-Ro Ferry”, *Proceedings of STAB2000*, Vol. 1, pp. 363-384.

Kat, J. de, Van't Veer, R. (2002), “Model Experiments and Simulations of a Damaged Ship with Air-Flow Taken into Account”, *Proceedings of ISSW 2002*.

Katayama. T., Ikeda, Y. (2005), “An Experimental Study of Fundamental Characteristics in Inflow Velocity From a Damage Opening”, *Proceedings of ISSW2005.*

Ruponen, P. (2006), “Pressure Correction Method for Simulation of Progressive Flooding and Internal Air Flows”, *Ship Technology Research*, 53, pp. 63-73.

Ruponen, P. (2007), “Progressive Flooding of a Damaged Passenger Ship”, PhD Dissertation, Helsinki University of Technology, Finland.

Ruponen, P., Sundell, T., Larmella, M. (2006). “Validation of a Simulation Method for Progressive Flooding”. *Proceedings of the 9th International Conference on the Stability of Ships and Ocean Vehicles (STAB’2006)*, Rio de Janeiro, Brasil.

Santos, T.A., Guedes Soares, C. (2001), “RoRo Ship Damage Stability Calculations Using

the Pressure Integration Technique", *International Shipbuilding Progress*, Vol. 48, Nº2, pp. 169-188.

Santos, T.A., Winkle, I.E., Guedes Soares, C. (2002), "Time Domain Modelling of the Transient Asymmetric Flooding of RoRo Ships", *Ocean Engineering*, Vol. 29, pp. 667-688.

Valanto, P. (2002), "Time-Dependent Survival Probability of a Damaged Passenger Ship - Volume 1", HSVA Report Nr. 620587.

Van 't Veer, R., Kat, J. de, Cojeen, H. (2002), "Large Passenger Ship Safety: Time to Sink", *Marine Technology*, Vol. 41 (2), pp 82-88.

Van 't Veer, R., Peters, B., Kat, J. de (2004), "Exploring the Influence of Different Arrangements of Semi- Watertight Spaces on Survivability of a Damaged Large Passenger Ship", *Proceedings of ISSW2004.*

Van't Veer, R., Kat, J. de (2000), "Experimental and Numerical Investigation on Progressive Flooding and Sloshing in Complex Compartment Geometry", *STAB2000*, Vol. 1, pp. 363-384.

Van't Veer, R., Kat, J. de, Cojeen, H. (2002), "Large Passenger Ship Safety: Time to Sink", *Proceedings of ISSW 2002*.

Walree F. van, Carette, N. (2008), "Benchmark study of numerical codes for the prediction of time to flood of ships: phase 2", *Proceedings of the 10th International Ship Stability Workshop*, Deajeon, Korea.

Walree, F. van, (2007). "Benchmark Study on Numerical Codes for the Prediction of Time to Flood of Ships - Phase I". Summary report to the ITTC Specialist Committee on Stability in Waves, 5 February, submitted by ITTC to IMO-SLF50.

Walree, F. van, Papanikolaou, A. (2007), "Benchmark Study of Numerical Codes for the Prediction of Time to Flood of Ships: Phase I", *Proceedings of the 9th International Ship Stability Workshop*, Hamburg, Germany.

Xia, J., Jensen, J.J., Pedersen, P.T. (1999), "A Dynamic Model for Roll Motion of Ships Due to Flooding", *Ship Technology Research*, Vol. 46, pp. 208-216.